Chemical Geology 482 (2018) 91–100

Contents lists available at ScienceDirect

Chemical Geology

journal homepage: www.elsevier.com/locate/chemgeo

Precipitation behaviour in the system Ca^{2+}-Co^{2+}-CO_3^{2-}-H_2O at ambient conditions — Amorphous phases and $CaCO_3$ polymorphs

Jorge González-López*, Ángeles Fernández-González, Amalia Jiménez

Department of Geology, University of Oviedo, Oviedo E-33005, Spain

ARTICLE INFO

Editor: Michael E. Böttcher

Keywords:
Calcium carbonate
Cobalt
Polymorphic transformations
Solvent-mediated transformations
Precipitation processes
Crystal growth

ABSTRACT

The crystallisation behaviour of calcium carbonate phases in the system Ca^{2+}-Co^{2+}-CO_3^{2-}-H_2O was examined in batch reactors. Experiments with different initial ratios of Co^{2+}/Ca^{2+} (from 0 to 1.0) in the aqueous solution were performed to examine precipitation and mineral transformations under ambient conditions. The solids recovered from the aqueous solution after different ageing periods (ranging from 5 min to 2 months after precipitation) were characterised by X-ray diffraction, transmission and scanning electron microscopy and EDX microanalyses. The evolution of the aqueous solutions was also followed by measuring their pH and their chemical composition by UVA–visible spectroscopy. Our experimental data indicate that there are two sequences of solvent-mediated transformations in aged carbonates, one involving Co-rich phases and another involving calcium carbonates. Both sequences are characterised by the initial formation of amorphous or poorly crystalline hydrated phases, which transform into crystalline and anhydrous phases with ageing *via* a dissolution and re-precipitation mechanism. The stability and solubility of the phases are concerned with the incorporation of Co in Ca-bearing phases and Ca in the Co-bearing phases. Co-rich carbonates evolve from a hydrated amorphous hydroxycarbonate ($Co_2CO_3(OH)_2 \cdot H_2O$) to the crystalline phase $Co_2CO_3(OH)_2$. The transformation from the amorphous to crystalline phase ($Co_2CO_3(OH)_2$) was increasingly delayed as the initial Co/Ca ratio lowered. The sequence of Ca carbonates is affected by the amounts of Co^{2+} in the initial solution, and instead of the sequence ACC (amorphous calcium carbonate) → vaterite (Vtr) → calcite (Cal) obtained for control experiments, we observed ACC → monohydrocalcite → aragonite (Arg). Moreover, the Co^{2+}/Ca^{2+} ratio controls the earliest calcium carbonate phases to appear and the subsequent polymorph transformation reactions. In terms of cobalt incorporation into the solids, monohydrocalcite and Arg incorporate a certain amount of cobalt into their crystalline structures. The thermodynamic solubility products of cobalt hydroxide carbonates (amorphous and crystalline) were determined. This experimental study advances the progress of understanding carbonate precipitation-dissolution-recrystallisation reactions under ambient conditions.

1. Introduction

Understanding the stability of the main phases is essential to predict the transformations that occur during rock-forming processes. Vast areas of the Earth's surface are covered by carbonate rocks, the main mineral in which is calcite (Cal). Furthermore, many carbonates are minerals with a particular economic interest. Although only a few carbonates are primary or secondary ores of, for example, Mg, Sr, Fe, and Co, carbonates, and specifically calcium carbonates, are among the most important industrial minerals because of their extensive and diverse uses in different industries: construction, glass, ceramic, plastic, paper, food, health and many others. Not only in nature but also in industry or laboratory conditions, most carbonates form by reaction-precipitation in aqueous solution, and therefore, the precipitation of carbonates from aqueous solution has been of great interest in the scientific literature.

A key aspect of calcium carbonate crystallisation is linked to the subject of $CaCO_3$ polymorphism and its hydrated phases. As is known, Cal is the stable phase at the Earth's surface conditions, but aragonite (Arg), vaterite (Vtr), monohydrocalcite, ikaite and amorphous calcium carbonate (ACC) can also form, influenced by biochemical and geochemical factors. For instance, some polymorphs (ACC, Arg, Vtr) are found in the skeletons of numerous organisms as several organic compounds can control the nucleation and growth of calcium carbonate polymorphs. However, geochemical conditions such as the presence of dissolved ions or salinity allow the metastable precipitation of calcium carbonates (Monohydrocalcite, ikaita, Arg). Among the numerous factors that influence the precipitation of calcium carbonate polymorphs,

* Corresponding author.
E-mail address: jgonzalez@geol.uniovi.es (J. González-López).

https://doi.org/10.1016/j.chemgeo.2018.02.003
Received 2 June 2017; Received in revised form 31 January 2018; Accepted 1 February 2018
Available online 06 February 2018

one of the most determinant is the presence of foreign ions or molecules in the aqueous solution from which the carbonate precipitates. For example, it has been observed that some divalent cations such as Mg^{2+} and Sr^{2+} favour Arg formation instead of Cal (Lippmann, 1973; Reddy and Wang, 1980); some oxyanions such as SO_4^{2-}, SeO_4^{2-} and CrO_4^{2-} favour the stabilisation of Vtr (Fernandez-Diaz et al., 2010; Fernandez-Gonzalez and Fernandez-Diaz, 2013; Sánchez-Pastor et al., 2011); other compounds such as different organic molecules stabilise ACC (see Gower and Odom, 2000).

In this work, we focus on the cobalt (II) ion and its influence in calcium carbonate precipitation. Experimental studies (Barber et al., 1975; Katsikopoulos et al., 2008; Wada et al., 1995) have shown that the presence of Co^{2+} in fresh or salt water in which $CaCO_3$ precipitates promotes the formation of amorphous phases and, at specific ratios of Co^{2+}/Ca^{2+}, favours the stabilisation of Arg. It has also been observed, at the molecular level, that Co^{2+} inhibits the nucleation and growth of Cal (Freij et al., 2004), and macroscopic studies suggest that it is incorporated into Cal surface layers, leading to the formation of a cobalt-bearing surface (González-López et al., 2017b). The published experimental studies are mainly based on precipitation, but the evolution of the precipitated phases and the eventual transformations that can occur in the aqueous solution after precipitation remain unstudied. In this study, we designed a set of experiments in which after precipitation in the system Ca^{2+}-Co^{2+}-CO_3^{2-}-H_2O, the precipitated solids were aged in the remaining aqueous solution under ambient conditions (temperature and atmospheric CO_2 partial pressure). The nature and crystallisation behaviour of the solids and the evolution of the aqueous solution chemistry with increasing reaction times were investigated. Furthermore, the thermodynamic solubility products of cobalt hydroxide carbonates (amorphous and crystalline) were also determined. The ageing precipitation experiments along with the solubility data obtained from this study provide crucial insight into the calcium carbonate polymorphic transformation processes that occur in presence of cobalt in an aqueous environment.

2. Materials and methods

2.1. Precipitation + ageing experiments

In this study, we have reproduced some of the precipitation experiments conducted by Katsikopoulos et al. (2008), in which two different solutions of ($CaCl_2$ + $CoCl_2$) and Na_2CO_3 were mixed at room temperature. In this work, 15 different proportions of Co^{2+}/Ca^{2+} were considered, and the solids were separated by filtration and characterised immediately after precipitation. Here, we have selected only 4 of the 15 experiments: those with high Co^{2+}/Ca^{2+} ratios in which the precipitation of a low-crystallinity phase (lcp) was reported to have precipitated together with calcium carbonate polymorphs. Moreover, in the present study, the precipitated solids were not immediately filtered, but instead, they were aged in the remaining water solution for different predetermined periods of time.

Table 1 shows the concentration of the initial aqueous solutions. The labelled E0 experiment (control experiment) was run to follow evolution of calcium carbonate from an aqueous solution free of cobalt.

Table 1
Initial aqueous solutions for the precipitation + aging experiments.

Exp	Aqueous solution 1		Aqueous solution 2	Ratio
	$CoCl_2 \cdot 6H_2O$ (M)	$CaCl_2$ (M)	Na_2CO_3 (M)	Co^{2+}/Ca^{2+}
E0	–	0.05	0.05	–
E1	0.02	0.05	0.05	0.4
E2	0.03	0.05	0.05	0.6
E3	0.05	0.05	0.05	1
E4	0.05	–	0.05	–

For each experiment, 50 mL of a 0.05 M aqueous solution of Na_2CO_3 was mixed with 50 mL of a ($CaCl_2$ + $CoCl_2$) aqueous solution in a polypropylene reactor of 100-mL capacity. After mixing, the reactor was sealed using plastic tape to prevent evaporation and was maintained at 25 ± 0.5 ° C under continuous stirring at 100 rpm by means of Teflon® -covered magnetic bar. All solutions were prepared with analytic grade (Panreac®) reactants and deionised Milli-Q® water.

For each experiment, a set of nine identical runs was conducted, and each one was stopped after a predetermined period of ageing. The nine considered ageing periods were 5 min, 1, 5, 24 and 48 h, and 4, 7, 30 and 60 days. After ageing, the solids were separated by filtering the aqueous solutions with a 0.45-μm Millipore® filter, rinsed with Milli-Q® water to avoid excess salts and dried at room temperature. Furthermore, the aqueous filtered phase was kept at 8 ° C in a refrigerator. Finally, both solid and aqueous phases were sampled for their analysis. Each run was repeated at least three times to check the reproducibility of the results.

2.2. Solid phases characterisation

After each experiment, a representative sample of the precipitated phase was selected and characterised by different instrumental techniques to determine its chemical and mineralogical composition, morphology, crystallinity and eventual evolution with ageing time. Solids were first analysed by powder X-ray diffraction (XRD) to identify the solid phases and determine their crystallinity. Moreover, in the case of the identified crystalline phases, the observed reflections were indexed, and the corresponding cell parameters calculated and refined.

The diffraction patterns were obtained by scanning from 5° to 80° of 2θ with a step size of 0.02° on a Philips X'PertPro diffractometer using Cu$K\alpha$ radiation. The instrument was periodically calibrated with an external Si standard. The collected diffractograms were processed with the X'Pert HighScore Plus (PANalytical B.V.) software.

The morphology and a first estimation of the composition of the precipitates were studied by scanning electron microscopy (SEM) in a JEOL 6610LV microscope equipped with an INCA Energy 350 microanalysis system (EDX) supplied with the Xmax 50 silicon drift detector (PentaFET, Oxford Instruments) fitted with an ultra-thin window that allows the detection of oxygen. Secondary and backscattering electron images allowed the detailed observation of the external morphology and the discrimination of possible compositional inhomogeneities on the solid surfaces. The microanalysis system provided a semi-quantitative chemical analysis of the precipitates. More precise quantitative chemical analyses were performed in a JEOL JEM-2100 transmission electron microscope equipped with an Energy Dispersive X-ray (EDX) micro-analyser.

2.3. Aqueous phase characterisation and modelling

The aqueous solutions were monitored for pH, alkalinity and cobalt and calcium concentrations for the entire reaction time. Both pH and alkalinity were immediately measured after filtration using a CRISON Compact Tritrator S equipped with a CRISON electrode, model 50-14T. The electrode was regularly calibrated with two CRISON buffer solutions of pH 4.01 and 7.

Cobalt and calcium concentrations were determined by UVA-visible spectroscopy in an AquaMate Vis Spectrophotometer (Thermo Scientific). Cobalt determination was performed by the Hach method 8078 with a wavelength of 620 nm, a precision of 95% (0.99–1.01 mg/L Co) and a sensitivity of 0.01 mg/L Co per the 0.010 absorbance change. Calcium analysis was conducted using the Spectroquant® method 14815 at a wavelength of 550 nm with a standard deviation of ± 1.5 mg/L Ca and a sensitivity of 1.4 mg/L Ca per 0.010 absorbance change.

From the analytical data, the aqueous phases of each experiment and for each specific ageing time were modelled with the geochemical code PHREEQC (Parkhurst and Appelo, 1999) and the phreeqcd.dat

database supplemented with the solubility products $K_{sp} = 10^{-7.91}$ of Vtr (Plummer and Busenberg, 1982) and $K_{sp} = 10^{-7.05}$ of monohydrocalcite (Kralj and Brecevic, 1995) and supplemented with the solubility products determined in this work.

2.4. Solubility measurements

The solubilities of the amorphous and crystalline cobalt hydroxide carbonates produced in the precipitation + ageing experiments are unknown. Since solubility is an important factor for interpreting the experimental results, specific dissolution experiments were performed with the aim of determining this aspect. For this purpose, two solids obtained from the E4 experiment at predetermined periods of time (24 h and 60 days) were used to determine the solubilities of the amorphous and crystalline cobalt hydroxide carbonates, respectively. In both cases, 0.5 g of the previously identified solid were placed in 200 mL of deionised Milli-Q® water at room temperature under constant stirring until equilibrium was reached. Equilibrium was tested by measuring the aqueous solution conductivity with a CRISON Micro-CM 2201 conductimeter until no changes in aqueous solution conductivity were detected.

After equilibration, analysis and modelling of the aqueous solutions were required to determine the solubility products and were performed as described in Section 2.3.

3. Results

3.1. Evolution of solids I: identification of phases and morphology

X-ray powder diffraction analyses (Fig. 1) show that after precipitation, the solid phases evolve during the measured ageing times. A summary of the identified phases for each experiment at the different ageing times is provided in Table 2 and described in detail below.

In the control experiment E0 (see Table 1 for initial fluid composition), the precipitate evolves from a mixture of Cal and Vtr, which is found 5 min after precipitation, to exclusively Cal. The progressive and complete transformation towards the final Cal occurs in approximately

Table 2
Identified phases by XRD for the different experiments and maturation times. Low crystallinity phase: lcp; calcite: c; aragonite: a, vaterite: v; monohydrocalcite: m and cobalt hydroxide carbonate: h. The dotted line represents the first clear appearance of aragonite. The straight line represents the first appearance of cobalt hydroxycarbonate.

Time	E0	E1	E2	E3	E4
5 min	v + c	lcp + c + a	lcp + a + c?	lcp	lcp
1 h	v + c	lcp + m + a	lcp + m	lcp	lcp
5 h	c	lcp + m + a	lcp + m	lcp	lcp
24 h	c	lcp + a + m	lcp + m + a	lcp	lcp
48 h	c	lcp + a	lcp + a	lcp + a	lcp
4 days	c	lcp + a	lcp + a	a + h	lcp + h
7 days	c	lcp + a	a + h	h + a	h
30 days	c	a + h	a + h	h + a	h
60 days	c	a + h	a + h	h + a	h

5 h. In a similar way, an initial amorphous cobalt hydroxide carbonate (lcp) precipitates at the early stages of the control experiment E4 (Table 2) and evolves to a crystalline phase (h) after four days. These results confirm that the phase transformation process is relatively fast at low temperature, which is in agreement with kinetic studies previously reported by González-López et al. (2016).

In the cases of experiments E1, E2 and E3, the solids undergo a more complex evolution during maturation. When cobalt is present, a low crystalline or amorphous phase immediately precipitates after mixing the parent solutions and is the dominant phase for the first 24 h. This low-crystallinity phase is the one identified by Katsikopoulos et al. (2008) as an amorphous cobalt hydroxycarbonate hydrate by IR spectroscopy. However, this amorphous phase is not the only one present in solids of experiments E1 and E2. Five minutes after precipitation, small reflections corresponding to Arg and Cal are also present in the diffractograms. Both are very minor phases, and the amount of crystalline Cal and Arg is even lower when there is more cobalt in the initial aqueous solution (*i.e.*, experiment E2). This is in good agreement with the observations of Katsikopoulos et al. (2008). SEM images show that Cal, when present, mainly presents spherical morphology with rounded surfaces in the zone of [001], and in some of the grains, it is possible to distinguish the vertex of the rhombohedron corresponding to the

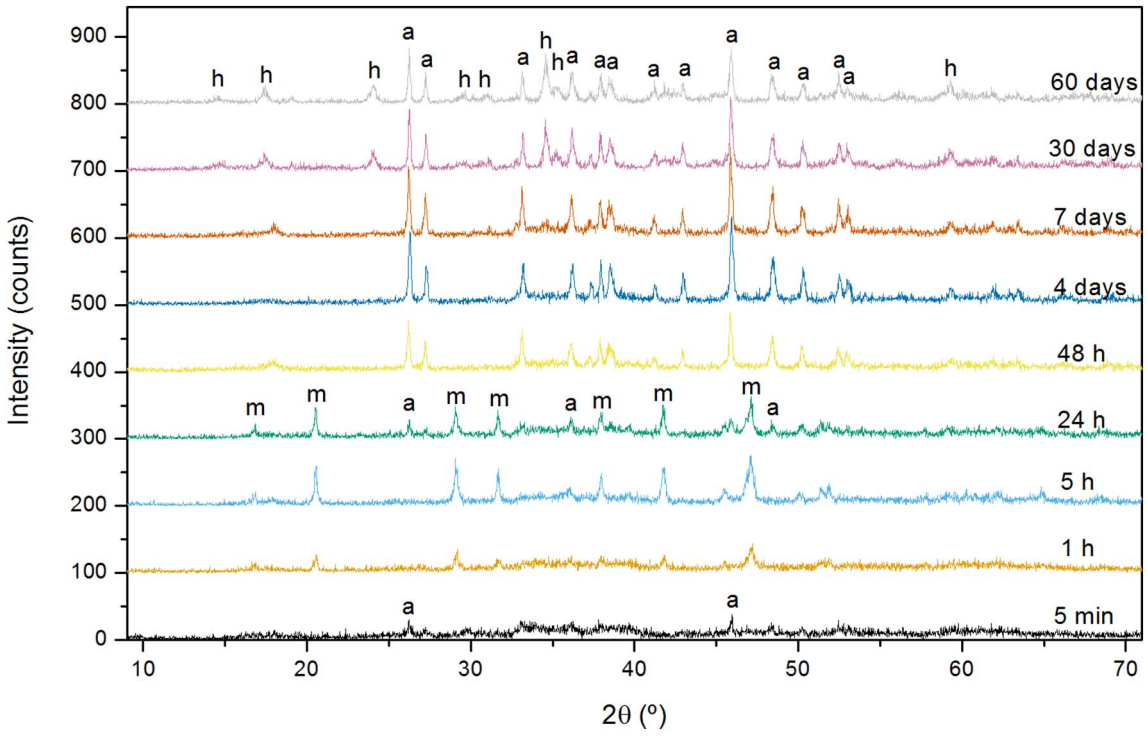

Fig. 1. Diffraction patterns for the E2 experiments ($Co^{2+}/Ca^{2+} = 0.6$). From bottom to top, reaction time increased. a: aragonite, m: monohydrocalcite and h: cobalt hydroxycarbonate.

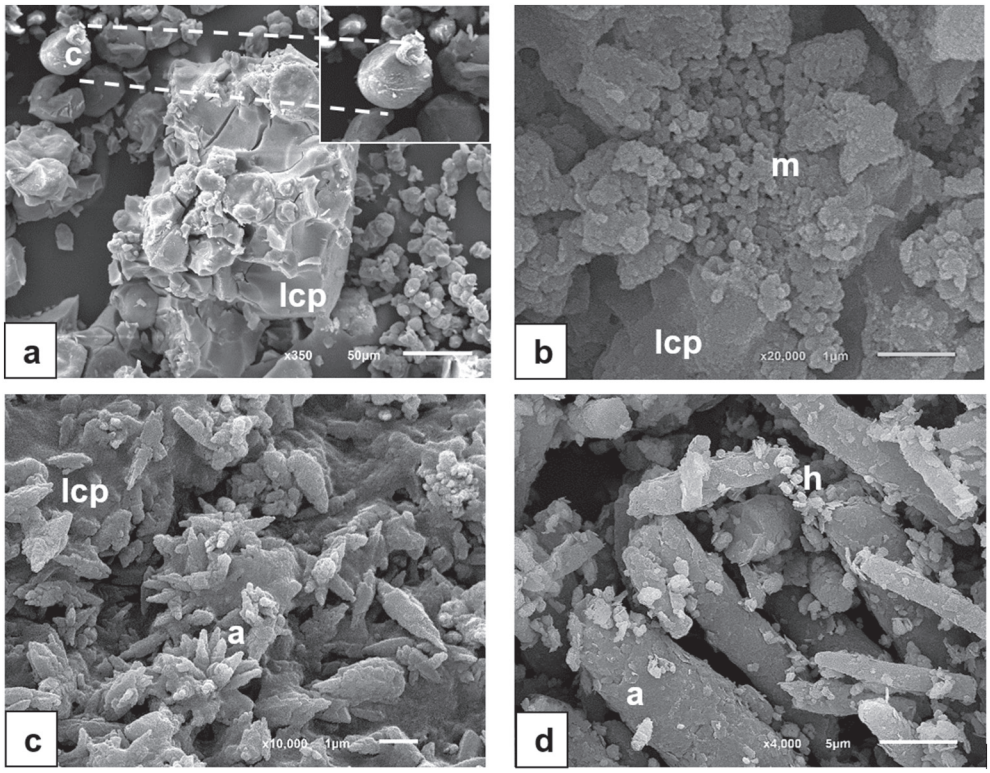

Fig. 2. SEM images of the precipitates formed in different experiments at different aging times. (a) Cal (c) crystals with the low-crystallinity phase (lcp) main phase corresponding to E2 experiment after 5 minutes. (b) Nanocrystals of monohydrocalcite (m) on the low-crystallinity phase (lcp) in experiment E1 5 hours after precipitation. (c) Abundant Arg aggregates (a) on the low-crystallinity phase (lcp) in experiment E1 after two days of maturation. (d) Arg rounded prismatic crystals (a) and $Co_2CO_3(OH)_2$ platelets (h) that appeared at the end of experiments and correspond to E2 after 1 month of ageing.

ternary axis. Fig. 2a shows some small aggregates of Cal together with the amorphous phase. Arg crystals could not be identified by its morphology in SEM images in samples aged for 5 min.

One hour after precipitation, new peaks in the diffractograms reveal the presence of monohydrocalcite ($CaCO_3 \cdot H_2O$) in E1 and E2, whereas Cal is no longer observed and Arg is present in only a very small amount in E2. As shown in Table 2, monohydrocalcite is present in both samples at least up to 1 day after precipitation. SEM images such as the picture in Fig. 2b also confirm that the amorphous phase is still important after one day. Monohydrocalcite is present as small rounded or elongated nanocrystals that tend to form aggregates in the amorphous phase as shown in Fig. 2b. Although an exhaustive quantitative study has not been performed, monohydrocalcite crystals are slightly more abundant in E1 than in E2.

If we increase ageing time, the reflections of monohydrocalcite become progressively less important in the diffractograms until their complete disappearance. The X-ray diffraction diagrams of samples E1 and E2 do not show any monohydrocalcite peak beyond two days of ageing. Conversely, the reflections corresponding to Arg become more important with ageing time. In fact, Arg is the main crystalline phase in samples E1, E2 and E3 from the second day after precipitation until the end of the experiments. Moreover, it is noteworthy that, as marked in Table 2, the first appearance of Arg is earlier for lower cobalt content in the initial aqueous solution. Under SEM, Arg crystals are seen to form star-like aggregates of prismatic crystals and in some of them, such as the detail in Fig. 2c,the pseudohexagonal twin that is frequently found in Arg is readily recognised.

Finally, cobalt hydroxide carbonate $Co_2CO_3(OH)_2$ reflections appear at the final stage of the reaction in experiments E1, E2 and E3. As seen in Table 2, (straight line) the first appearance of $Co_2CO_3(OH)_2$ occurs earlier in experiments with high Co^{2+}/Ca^{2+} ratios in the initial solutions. This phase appears as platelet-like crystals shown in Fig. 2d. Meanwhile, Arg crystals are frequently single prismatic crystals, and their sizes are substantially larger and show rounded corners and edges.

Given the foregoing descriptions, the evolution of the solids is concluded to be complex, and it is remarkable that the Oswald rule that is met in the control experiment in the absence of cobalt is not followed in the presence of cobalt.

3.2. Evolution of solids II: crystallinity and crystallographic parameters

A careful analysis of the X-ray diagrams offers supplementary information about the crystalline phases that were formed at the different ageing times. Reflections in the diffractograms corresponding to 5 minutes of ageing time show low intensity below 100 counts. Moreover, due to the abundant presence of the amorphous cobalt carbonate, the diffractograms corresponding to this ageing time are noisy. Although the identification of Arg and Cal at the early stages is possible and in the case of Cal, confirmed with SEM images, the quality of the diagrams does not allow any accurate determination of their crystallographic parameters. Table S1 (Supplementary material) shows the position and width (Full Width at Half Maximum) of the main peaks of each identified phase at the different ageing times.

For experiments in which the quality of the diffractograms allowed it, the reflections corresponding to Arg were indexed and the cell parameters refined. Fig. 3 shows that the cell volume of Arg is virtually the same for experiments E1, E2 and E3, and no appreciable changes with time are observed in any of these three experiments. On the other hand, the reflections of Arg are relatively well defined and sharp. The good crystallinity of Arg that can be deduced from the diffractograms is also confirmed by high-resolution transmission electron microscopy (HRTEM) images such as the one shown in Fig. 4a.

Reflections corresponding to monohydrocalcite in samples E1 and E2 are wide, and their positions vary slightly with ageing time and the initial compositions of the aqueous solutions. However, the main reflections can be indexed in the Space Group $P3_1$ and the refined cell volumes fit quite well with the value given by Taylor (1975) for this phase. However, as shown in the plot of Fig. 3, the cell volume of monohydrocalcite varies within a certain range and tends to increase with ageing time. The low quality of the nanocrystals that can be deduced from the observed broad peaks is also confirmed under TEM. Fig. 4b shows a representative high-resolution TEM image. As seen, the

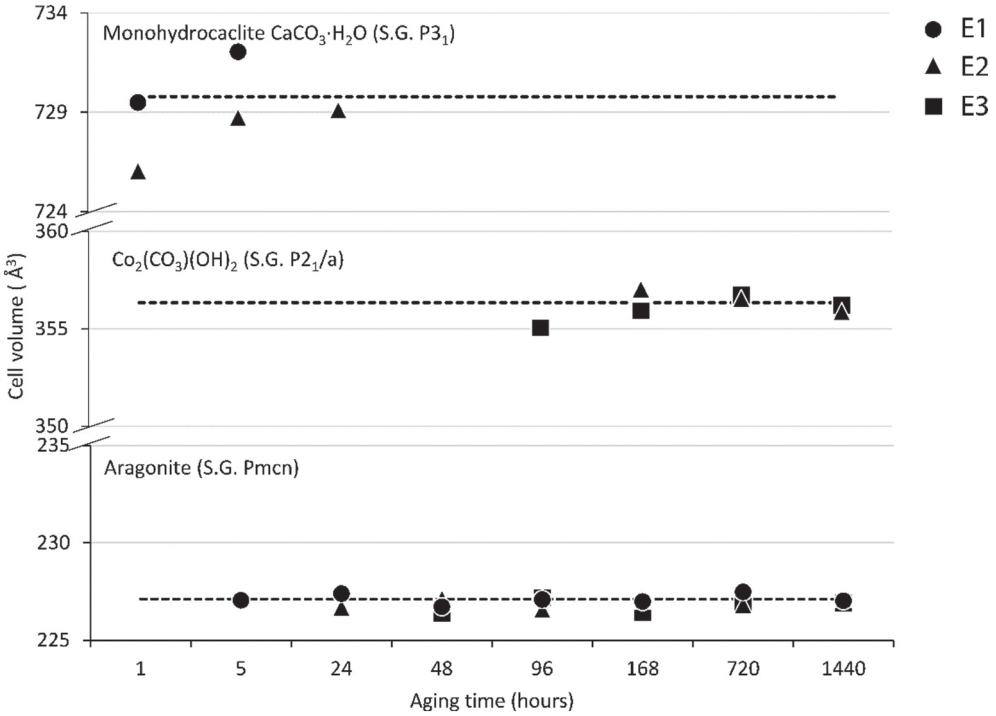

Fig. 3. Refined cell volumes of Arg, monohydrocalcite and $Co_2CO_3(OH)_2$ for the different experiments and ageing times. The dotted lines represent the reference value for the corresponding phase. See Tables S2, S3 and S4 in Supplementary material for the refined cell parameters.

coherence in monohydrocalcite crystals is not well preserved but each rounded-elongated entity of monohydrocalcite is formed by crystalline nano-domains misoriented with respect to their close neighbours.

In the diffractograms where cobalt hydroxycarbonate is identified, the corresponding reflexions are indexed in the Space Group $P2_1/a$ and the cell parameters determined and refined. Fig. 3 shows that these values agree with those published for $Co_2CO_3(OH)_2$ and remain quite constant. In general, the reflections observed for this phase are wide, which indicates that the crystallinity of $Co_2CO_3(OH)_2$ is poor. Moreover, the presence of nano-domains observed under TEM (see Fig. 4c) confirms the low crystallinity of this phase. Previous studies based on DFT simulations, suggest that the low crystallinity of $Co_2CO_3(OH)_2$ is related to its layered structure as a result of stacking disordered of layers with malachite- and rosasite-like structures (González-López et al., 2017a).

3.3. Evolution of solids III: chemical composition

Fig. 5 records the chemical composition of the different solid phases for the various ageing times in experiment E2. A similar behaviour is observed in samples E1 and E3. In general, phases are Co-rich or very Ca-rich. However, monohydrocalcite and also Arg incorporate a certain amount of cobalt. Moreover, the compositions of both phases change with ageing, and as seen, there is a tendency to purify, *i.e.*, to lose cobalt as time passes. According to the results presented in Section 3.2, the incorporation of cobalt in the crystal structure of Arg does not seem to greatly affect the quality of the X-ray diffractograms or the size of the cell parameters, but in the case of monohydrocalcite, lower amounts of Co mean an increase in the cell volume and better crystallinity.

The chemical composition of cobalt hydroxycarbonate is constant, and no impurities of calcium or any other ions are found. Cal seems not to incorporate cobalt, although it is necessary to remark here that the analysis of Cal, which appears only in the very early stages of ageing, is particularly complicated because Cal crystals are very rare and it is

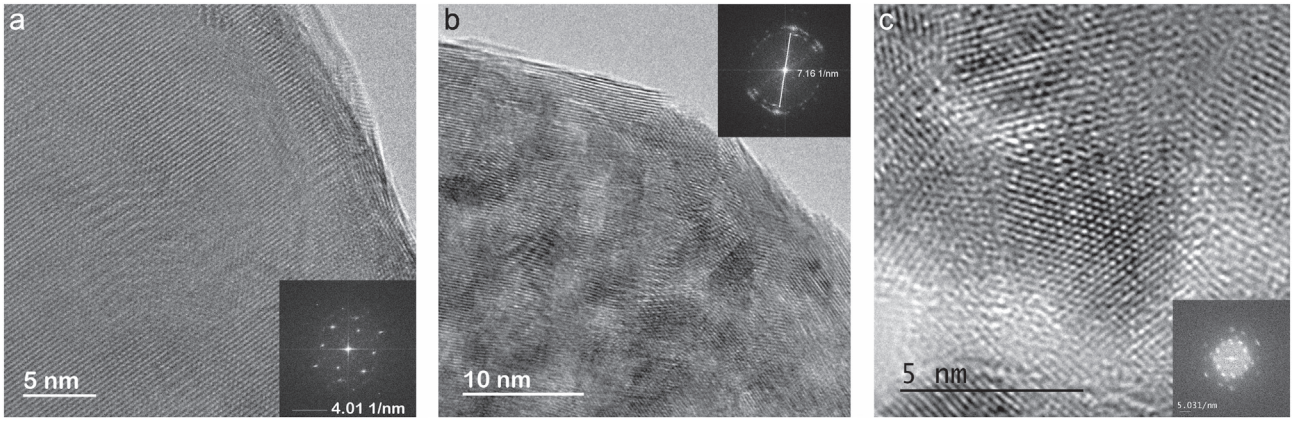

Fig. 4. High-resolution TEM images of representative crystals of (a) aragonite, (b) monohydrocalcite and (c) $Co_2CO_3(OH)_2$. The observed poor crystallinity of monohydrocalcite and $Co_2CO_3(OH)_2$ compared with the better quality of Arg agrees with the broadness of the corresponding peaks reported in Table S1.

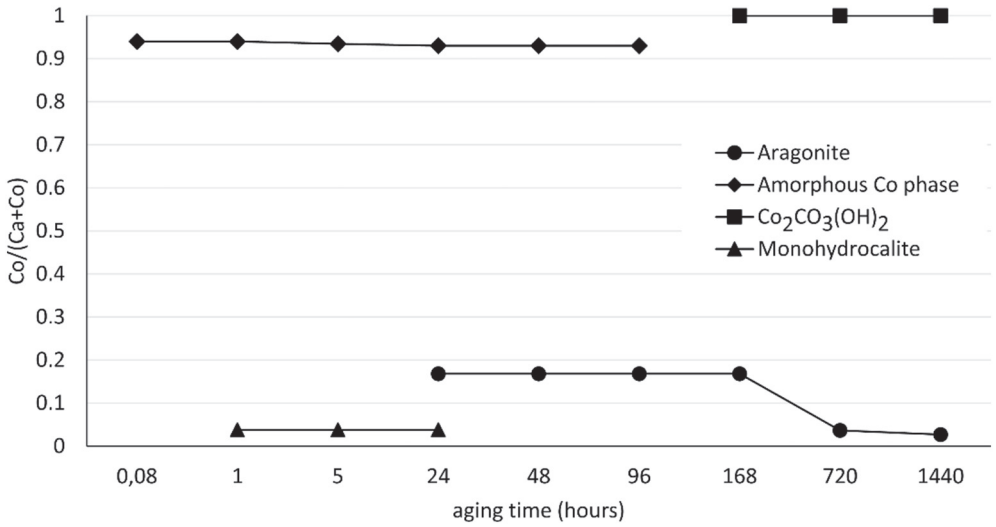

Fig. 5. Evolution of the ratio Co/(Ca + Co) with time in E2 for the different identified phases.

difficult to identify them under TEM.

The composition of the amorphous Co carbonate phase also evolves with ageing time. The initial Co ratio in the amorphous phase is 0.9 but progressively evolves to a Co-richer composition.

3.4. Determination of solubility

In the experiments conducted in this work, the solubility of phases is a key factor for the determination of the saturation indices and, therefore, for understanding the precipitation and the subsequent evolution of precipitated solids. In spite of some disagreements in the scientific literature, the solubilities of Cal, Arg, ACC and monohydrocalcite are well established and included in the main solubility databases. Unfortunately, to the authors' knowledge, the thermodynamic solubility products of $Co_2CO_3(OH)_2$ and the cobalt amorphous phase that precipitates from the very early stages are unknown and need to be investigated. The determination of the solubility is a difficult task, probably because of the complicated crystallisation behaviour of cobalt hydroxide carbonates under ambient conditions, which involves the instant precipitation of amorphous phases, the formation of a number of hydrate phases, the presence of pH-dependent carbonate species and a great amount of Co^{2+} aqueous complexes. Here, the solubility products of both amorphous and crystalline cobalt carbonates have been estimated assuming that the aqueous solution is in equilibrium with only one phase in experiment E4. Thus, solids obtained at the beginning (24 h) and at the end (60 days) are used to determine the solubility products of amorphous and crystalline cobalt hydroxide carbonate, respectively.

One obstacle in the determination of solubility of the amorphous phase is that its exact composition is unknown. According to previous studies based on attenuated total reflection infrared spectroscopy (ATR-IR) (Katsikopoulos et al., 2008; González-López et al., 2016), this amorphous phase is a hydrated cobalt carbonate whose composition is not fully determined. Thermogravimetric analysis combined with FTIR performed on this solid in the latter work shows that between 85 and 190 ° C, the sample undergoes a water loss that translates to approximately 8% of its total mass. At a higher temperature, approximately 240 ° C, the sample decomposes and loses (OH^-) and CO_2 simultaneously. A detailed study of this thermal analysis is beyond the scope of this work, but the results described above and the chemical analysis shown in the previous section agree fairly well with the stoichiometry $Co_2CO_3(OH)_2 \cdot H_2O$ that we have assumed for the amorphous phase.

The solubility values of the crystalline $Co_2CO_3(OH)_2$ and the amorphous $Co_2CO_3(OH)_2 \cdot H_2O$ obtained from the experiments described in the experimental Section 2.4 are very different. For the $Co_2CO_3(OH)_2$ crystalline phase, the constant solubility product reached values of $K_{sp} = 10^{-30.27}$ while for the amorphous $Co_2CO_3(OH)_2 \cdot H_2O$, the value was $K_{sp} = 10^{-28.28}$. The low solubility of the crystalline phase compared with the amorphous solid is expected considering the low stability of the amorphous carbonates. These solubility product values have been included in the database for the modelling of all the aqueous solutions and the determination of the saturation indices.

3.5. Aqueous solution evolution in precipitation + ageing experiments

Fig. 6 shows the concentration of total Ca and Co and the pH evolution of experiment E1 for the entire ageing period. The same general trend is also observed for experiments E2 and E3.

Immediately after mixing the initial aqueous solutions, the pH value is 9, but it quickly decreases due to the instantaneous precipitation of carbonates. For the first 5 h of ageing, the pH continues to fall to values of approximately 8. Then, the pH basically remains stable with a slight tendency to decrease and narrow fluctuations within the range of 7.8 to 8.1. The total concentration of Co and Ca also decreases strongly in the aqueous solution after mixing. It is noteworthy that, after an abrupt drop of concentration in the first 5 min, the concentration of both elements experiences a significant increase one hour after precipitation, from 12 ± 1 to 20 ± 3 ppm in the case of Co and from 270 ± 12 to 407 ± 20 ppm in the case of Ca. After this fleeting rise, the concentrations decrease and remain more or less stable with small fluctuations.

From these experimental data, the evolution of the aqueous solutions of all the experiments was modelled with PHREEQC (Parkhurst and Appelo, 1999), and the distribution of the aqueous species was determined. From these calculations, it is possible discern the total concentration of ions dissolved ($[Co^{2+}]_{dis}$ and $[Ca^{2+}]_{dis}$) from the activities of the dominant aqueous species (aCa^{2+} and aCo^{2+}). In all the experiments, $[Co^{2+}]_{dis}$ and $[Ca^{2+}]_{dis}$ are significantly higher than the activities of the corresponding ion during the entire interval of reaction time. The values of aCa^{2+} and aCo^{2+} obtained in experiment E1 are displayed in Fig. 6. As expected, the most significant changes in the solution chemistry occur in the first stages of reaction. After 5 min of reaction, significant decreases of aCa^{2+} and aCo^{2+} indicate that they were removed from the initial solution. After 1 h of reaction, $[Co^{2+}]$ and $[Ca^{2+}]$ are incorporated again into the solution as a result of the dissolution of phases precipitated previously. For prolonged reaction times, $[Ca^{2+}]$ decreases and remain more or less stable with small fluctuations as a result of the precipitation of calcium carbonate phases.

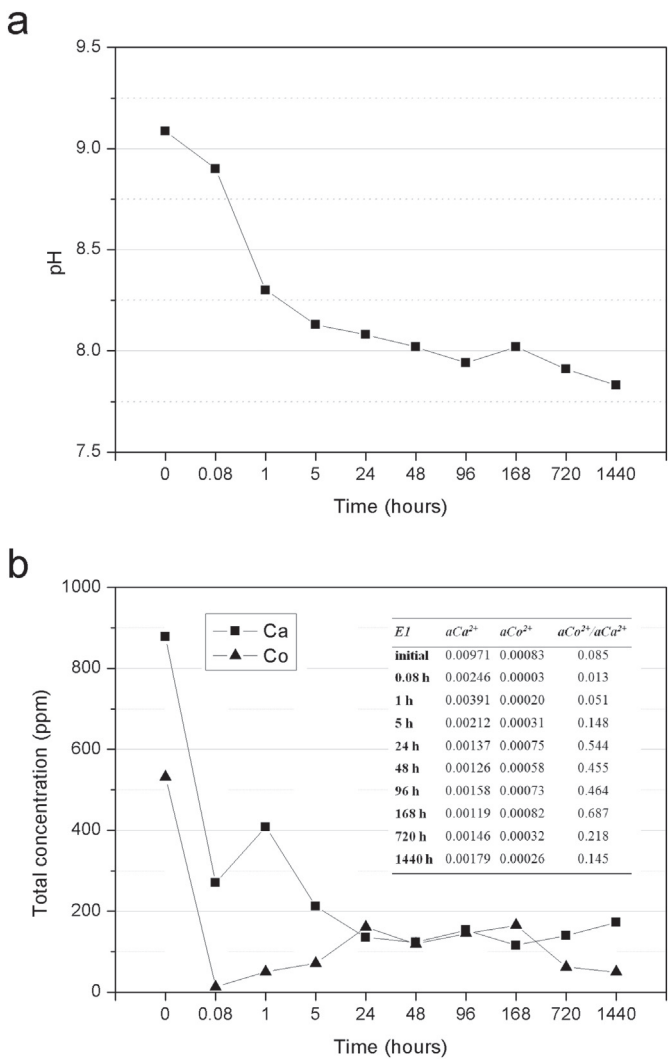

Fig. 6. pH (a) and total concentration of Co and Ca measured in experiment E1 during aging (b). The first point corresponds to the moment immediately after mixing, *i.e.*, to zero ageing time.

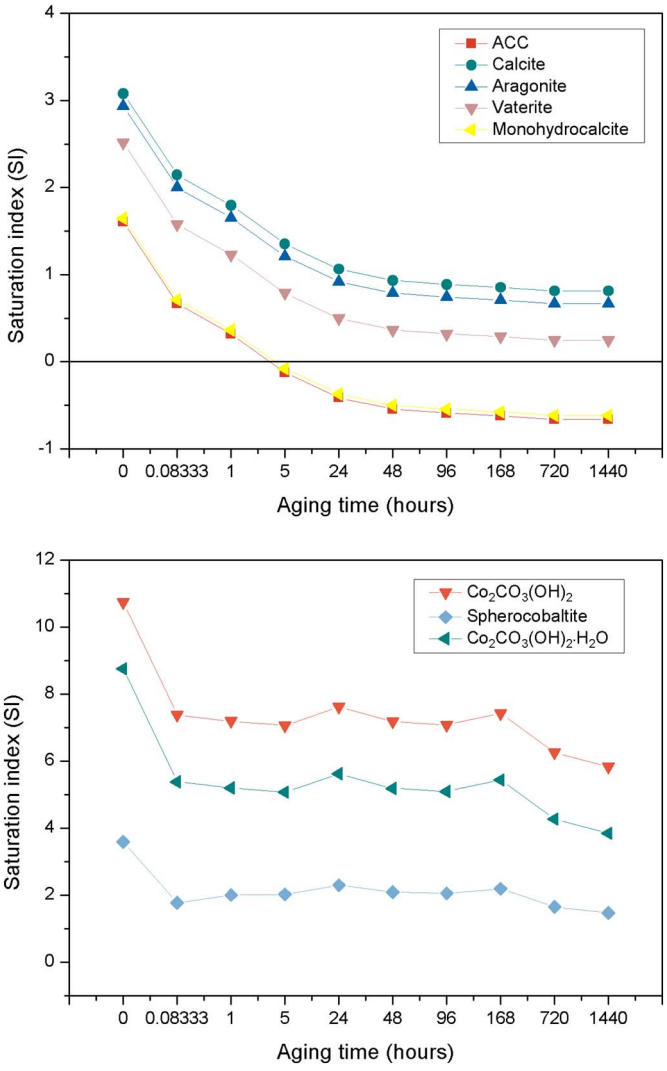

Fig. 7. Evolution of saturation indexes of the different solid phases with aging time in experiment E1.

However, $[Co^{2+}]$ increases up to 1 day and remain stable to decrease after 7 days of reaction as a result of the precipitation/dissolution reactions.

4. Discussion

The results of the experiments described in this work can be discussed in the framework of the crystallisation of carbonates by chemical reaction in aqueous solutions under ambient conditions. The precipitation behaviour and the subsequent evolution of precipitated solids in the Ca^{2+}-Co^{2+}-CO_3^{2-}-H_2O system are clearly complex and depend on multiple thermodynamic and kinetic factors. The different data achieved from diverse techniques permit us to propose the following sequence of events, which is controlled by the Co/Ca ratio in the fluid phase. In the sequence of solids produced from the initial aqueous solutions, two branches can be considered: (i) Co-rich solid formation and (ii) calcium carbonate formation.

4.1. First stages: precipitation and initial ageing period

The formation of amorphous $Co_2CO_3(OH)_2 \cdot H_2O$ is detected at the first stages of reaction in all experiments conducted with Co-bearing solutions (Figs. 1 and 2). However, such an amorphous phase remains for two days in E3 and is prolonged up to seven days in E1. Note here that in experiment E4, which contains only cobalt and carbonate as reactants, the amorphous $Co_2CO_3(OH)_2 \cdot H_2O$ appears as the only phase up to two days of reaction, however it is also detected along the crystalline phase up to four days. Along with this phase, different calcium carbonates have been identified in all the experiments conducted with Ca-bearing solutions. By comparing results obtained in all the experiments (see Table 2), the observed difference in the stability of the amorphous cobalt-bearing phase is more likely related to cobalt content in the reactive solutions than to competitive formation of other calcium carbonate phases.

To evaluate the stability or metastability of phases identified in the present experiments, saturation indices have been estimated by using PHREEQC code. From these calculations, it was possible to determine that the initial aqueous solutions were highly supersaturated with respect to a considerable number of solid phases (Fig. 7): Cal, Arg, Vtr, monohydrocalcite, spherocobaltite, $Co_2CO_3(OH)_2$ and amorphous $Co_2CO_3(OH)_2 \cdot H_2O$. Any of these phases could precipitate, but the saturation indices of crystalline $Co_2CO_3(OH)_2$ and amorphous $Co_2CO_3(OH)_2 \cdot H_2O$ are higher by far than the saturation indices of the different calcium carbonates. The precipitation of unknown intermediate Co-Ca carbonates with the same or different crystal structures would also be possible. However, there are no data in the scientific literature about these potential intermediate compounds with the exception of the $(Co,Ca)CO_3$ solid solutions (González-López et al., 2014),

which do not precipitate here. Fig. 7 also shows the evolution of the saturation indices of the different pure solid phases that are considered in experiment E1. Similar tendencies are observed in experiments E2 and E3.

The saturation index of $Co_2CO_3(OH)_2$ is especially high according to the very low solubility determined in this work ($K_{sp} = 10^{-30.27}$), and it is the best candidate to precipitate. Nevertheless, the first precipitated solid is the amorphous $Co_2CO_3(OH)_2 \cdot H_2O$ phase. In agreement with previous work (González-López et al., 2016; Rinaldi-Montes et al., 2017), $Co_2CO_3(OH)_2$ crystallises in water solutions from its amorphous precursor ($Co_2CO_3(OH)_2 \cdot H_2O$) *via* a dissolution-reprecipitation mechanism. Thus, the metastability of the amorphous $Co_2CO_3(OH)_2 \cdot H_2O$ phase can be attributed to the structural water connected to Co ions, which delays the process of dehydration and transformation (González-López et al., 2016). The low hydration energy of and more specifically the long half-life for water exchange of Co^{2+} (rate constant for water exchange $K_w = 2 \cdot 10^6\ s^{-1}$), data given by Margerum et al. (1978) compared for example with Ca^{2+} ($K_w = 2 \cdot 10^8\ s^{-1}$; Margerum et al., 1978) explain the difficulty for Co in forming anhydrous carbonate at room temperature. The same interpretation is valid to explain the slow kinetic of the cobalt crystaline anhydrous phase when compared to the rapid transformation of ACC into crystalline calcium carbonate.

The precipitation of amorphous precursors is common in many carbonate-water systems and has been extensively observed and explained in the literature (see e.g. Addadi et al., 2003; Giuffre et al., 2015; Loste et al., 2003; Pina, 2015; Purgstaller et al., 2017; Rodriguez-Navarro et al., 2016, 2015 and references therein). It is known from previous studies that calcium carbonate precipitates under similar conditions to those of the control experiment E0 (see Table 1), and it evolves from a mixture of Cal and Vtr, which in this case is found 5 min after precipitation, to exclusively Cal (Fernandez-Diaz et al., 2010). The progressive and complete transformation towards the final Cal occurs in approximately 4 hours *via* a dissolution-reprecipitation mechanism (Ogino et al., 1987). The very early stages of this process, before the formation of the Vtr-Cal mixture, are still under discussion and are beyond the scope of this work.

On the other hand, because the system is far from equilibrium, the precipitation is fast, and the amorphous cobalt solid incorporates small amounts of Ca present in the aqueous solution, as seen in Fig. 5. Moreover, under the conditions explored in our experiments, the precipitation of amorphous calcium carbonate (ACC) might precipitate in the first instances. Although we have not found any evidence of the occurrence of ACC, its presence in the initial stages of the process cannot be dismissed. The initial phase is, then, a mixture of amorphous calcium carbonate and amorphous cobalt hydroxycarbonate. Together with the very abundant amorphous phase, minor amounts of Cal and Arg are identified by XRD (Fig. 1) and observed by SEM images (Fig. 2). Furthermore, slight decreases in pH, accompanied by drastic decreases in both aCa^{2+} and aCo^{2+} within the first 5 min of reaction time (Fig. 6) are in good agreement with the precipitation of cobalt and calcium-bearing phases and the decreases of the saturation indices of all the solid phases (Fig. 7) in the same interval of time.

Cal, which grows as single crystals (Fig. 2a), is very rare, and it is not detected after one hour of ageing time. The dissolution of this stable phase is hard to explain but can be understood if one considers the evolution of the chemical solution: After 5 min of reaction time, approximately 93% of the aCo^{2+} (see Fig. 6) is removed from the solution due, at least in part, to the precipitation of amorphous $Co_2CO_3(OH)_2 \cdot H_2O$. As shown in Fig. 7, the system is still supersaturated with respect to all phases. Under such conditions far from equilibrium, the incorporation of small amounts of Co^{2+} ions in the Cal crystal structure cannot be completely excluded. In fact, the adsorption of cobalt ions, with an ionic ratio (0.78 Å) lower than that of calcium (0.99 Å), would significantly distort the Cal lattice, involving an increase of its free energy at least affecting the surface of the crystal. The increase in free energy produces an increase of solubility that would facilitate the dissolution of Cal. The permanence of Arg instead of thermodynamically more stable Cal can be explained by considering the solubility of both phases. Bearing in mind that the solubilities of Cal and Arg are similar, that of Co-bearing Cal can be higher than that of pure Arg, and hence, the latter remains in the system. Busenberg and Plummer (1985) have reported a similar behaviour for calcite doped with sulphate. They found that calcites with low sulphate contents (~1% molar) were more soluble than pure calcite, and calcites containing higher amounts of sulphate (more than 3% mole) were more soluble than pure aragonite. Here, the driving forces for the precipitation of calcium carbonates polymorphs can be directly related to the difference in solubility of Co-calcium carbonate phases. The dissolution of Cal produces an increase of aCa^{2+}/aCo^{2+} ratio after 1 h of reaction (see Fig. 6) since such process is involved in the solvent mediated transformation of Co-bearing calcite into pure Arg. Thus, the presence of cobalt ions plays a key role in the dissolution/precipitation reactions involving calcium carbonate phases.

4.2. Ageing II: intermediate time of ageing

One of the most surprising results of this work is the formation of monohydrocalcite in the ageing period from 1 h to 1 day in experiments E1 and E2. The identification of monohydrocalcite from the X-ray diffraction analysis is reliable, although the crystals show poor crystallinity, as deduced from their wide reflections in X-ray diffraction analysis (see FWHM values of monohydrocalcite in Table S1) and incorporate small amounts of Co, which could modify the solubility of this phase.

Monohydrocalcite is a non-stable phase whose crystallisation in nature under ambient conditions has been associated with the presence of Mg^{2+} (Nishiyama et al., 2013). Different authors (Liu et al., 2013; Rodriguez-Blanco et al., 2014; Purgstaller et al., 2017; Zhang et al., 2012) have observed that monohydrocalcite can form from a Mg-bearing amorphous calcium carbonate precursor, which transforms into monohydrocalcite via a nucleation-controlled reaction. In this case, the role of Co^{2+} would be comparable to that observed for Mg^{2+}. The analogous behaviour of Co^{2+} and Mg^{2+} in aqueous solution and their similar hydration energies and the half-lives of their hydrates justify their equal roles in the formation of monohydrocalcite. As noted by Rodriguez-Blanco et al. (2014) for the case of magnesium, the formation of monohydrocalcite occurs only in a certain range of intermediate $Mg^{2+}_{aq}/Ca^{2+}_{aq}$ ratios. Conversely, Purgstaller et al. (2017) propose the formation of monohydrocalcite when elevated prevailing aMg^{2+}/aCa^{2+} inhibits the growth of Cal. Here, the aCo^{2+}/aCa^{2+} ratios in the initial solutions of E1 and E2 are 0.085 and 0.139 respectively, and could explain the occurrence of monohydrocalcite in both experiments from the Cal detected at the beginning of the reaction (see Section 4.1). The mechanism of such transformation involves precipitation/dissolution reactions, in which the solubility of the cobalt-bearing monohydrocalcite phase plays a key role. Fig. 7 shows that the precipitation of monohydrocalcite begins when the system is supersaturated with respect to this phase (after 1 h of reaction). Nevertheless, monohydrocalcite precipitates after longer periods of reaction (24 h) as deduced from XRD (see Fig. 1) in spite of the expected dissolution after 5 h (Fig. 7). The permanence of this phase could be explained by considering a lower solubility of Co-monohydrocalcite than pure-monohydrocalcite. However, it would be necessary to carry out experimental studies similar to those of Busenberg and Plummer (1985) to verify possible fluctuations of solubility as a function of the concentration of cobalt in monohydrocalcite.In experiment E3, monohydrocalcite was likely not formed due to the high aCo^{2+}/aCa^{2+} ratio (2.018) in the initial solutions, which explain the inhibition of nucleation and growth of both Cal (Barber et al., 1975; Freij et al., 2004) as well as monohydrocalcite.

After one day of ageing, we have identified amorphous Co-

hydroxycarbonate (in experiment E3) or a mixture of it and a small amount of monohydrocalcite (in experiments E1 and E2). Both phases are metastable and the system should evolve towards equilibrium, *i.e.*, towards more stable phases. The process by which intermediate phases such as monohydrocalcite transform into a more stable calcium carbonate polymorph is under debate. More specifically, the transformation of monohydrocalcite into Arg in the presence of Mg^{2+} has been studied by different authors, and it is considered to be a dissolution-precipitation process involving the dehydration of monohydrocalcite (Liu et al., 2013; Rodriguez-Blanco et al., 2014; Zhang et al., 2012). The same evolution is observed here in the presence of Co^{2+}. After two days of ageing time, the SEM images show that small monohydrocalcite particles aggregate and finally form Arg. These steps are very similar to those described by Liu et al. (2013) for the monohydrocalcite-Arg transformation in the presence of Mg^{2+}.

Meanwhile, the ageing of amorphous $Co_2CO_3(OH)_2 \cdot H_2O$ results in its transformation into crystalline $Co_2CO_3(OH)_2$ through a dissolution-recrystallisation process that also involves dehydration and an internal structural reorganisation within the individual nanoparticles of the crystalline phase, as was fully discussed in a previous studies (González-López et al., 2016). The phase transformation from cobalt amorphous into crystalline $Co_2CO_3(OH)_2$ occurs after more prolonged periods of time than those needed when monohydrocalcite transform into Arg. Moreover, the metastability of amorphous $Co_2CO_3(OH)_2 \cdot H_2O$ is determined by the cobalt content in the aqueous phase; *i.e.*, the metastable amorphous phase remains during shorter intervals of reaction at higher Co/Ca ratios in the initial aqueous solution (see Table 2). Because the ions dissolved in the fluid phase are the same in all experiments, the increase of aCo^{2+} (0.00134, 0.00382 and 0.00954 in E1, E2 and E3 respectively) imply greater availability of cobalt ions to attract water molecules from the hydrated amorphous cobalt phase. Moreover, an increase of cobalt concentration (higher Co/Ca ratio) involves a decrease in both equivalent conductivity and ion mobility, which are factors that could favour a faster transformation from amorphous to crystalline cobalt-bearing phase.

The permanence of aragonite instead a more stable phase, such as calcite, can be explained by considering the effect of foreign ions in the solution on the solubility of calcium carbonate polymorphs (Busenberg and Plummer, 1985). Here, the incorporation of cobalt in aragonite (see Fig. 5) involves a lower solubility of Co Arg than Cal. A similar behaviour has been described by Fernandez-Diaz et al. (2010) for the stabilisation of vaterite in the presence of sulphate. Other explanations are also pausibles such as crystal size or a high sobresaturation rate, however, an exhaustive study of the extent to which Co^{2+} modifies calcium carbonates solubility is beyond the scope of this work.

4.3. Final stages of ageing

After the transformation of monohydrocalcite, the newly formed Arg evolves. The first crystals of Arg contain appreciable amounts of cobalt, up to 4% of Co atoms, with respect to Ca. With ageing time, Arg crystals grow and become purer, and their crystallinity increases. The incorporation of Co^{2+} ions into the crystal structure of Arg is very unfavourable from a thermodynamic point of view (González-López et al., 2014). However, Arg can incorporate cobalt when it precipitates at very high supersaturation in the presence of Co^{2+} in the fluid phase. High amounts of Co^{2+} up to 0.16 mole fraction of Co, have been observed in experimentally grown Arg (Katsikopoulos et al., 2008). It is still unknown whether Co^{2+} (or a Co^{2+} complex) metastably substitutes for Ca^{2+} in the crystal structure of Arg or whether cobalt is in a non-structural position within the crystal structure. The incorporation of cobalt (or one of its complexes) in the surface of the Arg produces local tensions in the crystalline network that increase the "lattice energy," producing an increase in the solubility of the Co-rich Arg phase. Over time, dissolution/precipitation reactions at the interface of Arg would favour the release of cobalt ions from the structure of Arg, which becomes purer while its crystallinity increases (see Fig. 5 and FWHM values for Arg in Table S1). The dissolution and re-precipitation of impure phases (mainly Arg and monohydrocalcite) imply small fluctuations in the amounts of Ca and Co in the aqueous solution that are observed in Fig. 6 and, as a consequence, in the saturation indices as shown in Fig. 7. The fluctuations affect the kinetic of the transformations during ageing, but finally, the system evolves to pure or almost pure Arg and pure $Co_2CO_3(OH)_2$. The presence of Arg instead of the more stable Cal in this final stage is explained by the inhibition that cobalt exerts on the nucleation and growth of Cal (Barber et al., 1975; Freij et al., 2004) and has been discussed in the scientific literature.

5. Conclusions

The experimental study of the precipitation and ageing of solids at room temperature in the system Ca^{2+}-Co^{2+}-CO_3^{2-}-H_2O is crucial to understand the influence of Co^{2+} on the precipitation of calcium carbonate. Moreover, the presence of cobalt has an effect on the phase transformation processes that occur in calcium and cobalt carbonates after precipitation under ambient conditions.

In the presence of Co^{2+}, the normal sequence of calcium carbonate crystallisation that follows the Ostwald's step rule is drastically modified. Instead of the known sequence of ACC → Vtr → Cal, in the presence of Co^{2+} the general sequence is ACC → monohydrocalcite → Arg. If the Co^{2+}/Ca^{2+} ratio is higher than 0.6, the intermediate monohydrocalcite does not form, and the sequence is ACC → Arg. Simultaneous with this sequence, the precipitation of $Co_2CO_3(OH)_2$ occurs only after ageing a low-crystallinity $Co_2CO_3(OH)_2 \cdot H_2O$ precipitate. In both crystallisation sequences, cobalt carbonates and calcium carbonates, the earliest phases to appear tend to be more chemically impure and less crystalline.

The two sequences that culminate in a mixture of Arg and $Co_2CO_3(OH)_2$ imply the dehydration and its transformation in crystalline phases. The kinetics of these transformations are conditioned by the long half-life for water exchange of the cobalt ion. A similar effect has been observed by diverse authors (Liu et al., 2013; Rodriguez-Blanco et al., 2014; Zhang et al., 2012) in the case of Mg^{2+}, with a comparable half-life for water exchange.

Moreover, at the early stages of ageing, the high supersaturation levels in which the experiments start permit the incorporation of appreciable amounts of cobalt into the calcium carbonate (monohydrocalcite, Arg and probably in Cal) crystal structures. However, as supersaturation decreases and the dissolution-reprecipitation of solid phases progresses, Arg becomes progressively more pure and crystalline. Finally, the inhibitory effect of Co^{2+} on Cal nucleation and growth that has been observed in previous studies at the molecular level (Freij et al., 2004) is also connected with the hydration of this cation and prevents the formation of Cal even after a relatively long period of reaction.

This study provides new insights into the potential mechanism responsible for the calcium carbonate polymorphic transformation processes in natural multicomponent systems. In addition to amorphous substances, $CaCO_3$ polymorphs as well as hydrated phases are modified by cobalt, and it can have a great impact over global processes on the Earth. For instance, biogenic precipitation of calcium carbonates, which is the main source of carbonates on the planet, can be altered in seawater or groundwaters by the presence of cobalt. Finally, dissolved cobalt may affect further processes after precipitation, such as diagenesis or dissolution under environmental conditions.

Acknowledgements

This research was supported by MINECO-Spain, (grantsCGL2013-47988-C2-2-P andCGL2016-77138-C2-2-P). J. González-López acknowledges a FPI fellowship from the Spanish MICINN (grantCGL2010-20134-CO2-02). We thank the Editor, professor Michael Böttcher and

two anonymous reviewers for their detailed comments and valuable suggestions that greatly improved this manuscript.

Appendix A. Supplementary data

Supplementary data to this article can be found online at https://doi.org/10.1016/j.chemgeo.2018.02.003.

References

Addadi, L., Raz, S., Weiner, S., 2003. Taking advantage of disorder: amorphous calcium carbonate and its roles in biomineralization. Adv. Mater. 15, 959–970. http://dx.doi.org/10.1002/adma.200300381.

Barber, D.M., Malone, P.G., Larson, R.J., 1975. The effect of cobalt ion on nucleation of calcium-carbonate polymorphs. Chem. Geol. 16, 239–241.

Busenberg, E., Plummer, N., 1985. Kinetic and thermodynamic factors controlling the distribution of SO_3^{2-} and Na^+ in calcites and selected aragonites. Geochim. Cosmochim. Acta 49, 713–725. http://dx.doi.org/10.1016/0016-7037(85)90166-8.

Fernandez-Diaz, L., Fernandez-Gonzalez, A., Prieto, M., 2010. The role of sulfate groups in controlling $CaCO_3$ polymorphism. Geochim. Cosmochim. Acta 74, 6064–6076. http://dx.doi.org/10.1016/j.gca.2010.08.010.

Fernandez-Gonzalez, A., Fernandez-Diaz, L., 2013. Growth of calcium carbonate in the presence of Se(VI) in silica hydrogel. Am. Mineral. 98, 1824–1833. http://dx.doi.org/10.2138/am.2013.4397.

Freij, S.J., Putnis, A., Astilleros, J., 2004. Nanoscale observations of the effect of cobalt on calcite growth and dissolution. J. Cryst. Growth 267, 288–300.

Giuffre, A.J., Gagnon, A.C., De Yoreo, J.J., Dove, P.M., 2015. Isotopic tracer evidence for the amorphous calcium carbonate to calcite transformation by dissolution-re-precipitation. Geochim. Cosmochim. Acta 165, 407–417. http://dx.doi.org/10.1016/j.gca.2015.06.002.

González-López, J., Cockcroft, J., Fernández-González, A., Jiménez, A., Grau-Crespo, R., 2017a. Crystal structure of cobalt hydroxide carbonate $Co_2CO_3(OH)_2$: density functional theory and X-ray diffraction investigation. Acta Crystallogr. B 73, 868–873. http://dx.doi.org/10.1107/S2052520617007983.

González-López, J., Fernández-González, A., Jiménez, A., 2016. Crystallization of nanostructured cobalt hydroxide carbonate at ambient conditions: a key precursor of Co_3O_4. Min. Mag. 80, 995–1011. http://dx.doi.org/10.1180/minmag.2016.080.036.

González-López, J., Fernández-González, A., Jiménez, A., Godelitsas, A., Ladas, S., Provatas, G., Lagogiannis, A., Pasias, I.N., Thomaidis, N.S., Prieto, M., 2017b. Dissolution and sorption processes on the surface of calcite in the presence of high Co^{2+} concentration. Minerals 7(2). http://dx.doi.org/10.3390/min7020023.

González-López, J., Ruiz-Hernández, S.E., Fernández-González, A., Jiménez, A., De Leeuw, N.H., Grau-Crespo, R., 2014. Cobalt incorporation in calcite: thermochemistry of $(Ca,Co)CO_3$ solid solutions from density functional theory simulations. Geochim. Cosmochim. Acta 142, 205–216. http://dx.doi.org/10.1016/j.gca.2014.07.026.

Gower, L.B., Odom, D.J., 2000. Deposition of calcium carbonate films by a polymer-induced liquid-precursor (PILP) process. J. Cryst. Growth 210, 719–734. http://dx.doi.org/10.1016/s0022-0248(99)00749-6.

Katsikopoulos, D., Fernández-González, A., Prieto, A.C., Prieto, M., 2008. Co-crystallization of Co (II) with calcite: implications for the mobility of cobalt in aqueous environments. Chem. Geol. 254, 87–100.

Kralj, D., Brecevic, L., 1995. Dissolution kinetics and solubility of calcium-carbonate monohydrate. Colloid. Surf. A 96, 287–293. http://dx.doi.org/10.1016/0927-7757(94)03063-6.

Lippmann, F., 1973. Sedimentary Carbonate Minerals. Springer-Verlag Berlin.

Liu, R., Liu, F., Zhao, S., Su, Y., Wang, D., Shen, Q., 2013. Crystallization and oriented attachment of monohydrocalcite and its crystalline phase transformation. CrystEngComm 15, 509–515. http://dx.doi.org/10.1039/c2ce26562a.

Loste, E., Wilson, R.M., Seshadri, R., Meldrum, F.C., 2003. The role of magnesium in stabilising amorphous calcium carbonate and controlling calcite morphologies. J. Cryst. Growth 254, 206–218. http://dx.doi.org/10.1016/s0022-0248(03)01153-9.

Margerum, D.W., Cayley, G.R., Weatherburn, D.C., Pagenkopf, G.K., 1978. American Chemical Society, Washington, D.C.

Nishiyama, R., Munemoto, T., Fukushi, K., 2013. Formation condition of monohydrocalcite from $CaCl_2$-$MgCl_2$-Na_2CO_3 solutions. Geochim. Cosmochim. Acta 100, 217–231. http://dx.doi.org/10.1016/j.gca.2012.09.002.

Ogino, T., Suzuki, T., Sawada, K., 1987. The formation and transformation mechanism of calcium-carbonate in water. Geochim. Cosmochim. Acta 51 (10), 2757–2767. http://dx.doi.org/10.1016/0016-7037(87)90155-4.

Parkhurst, D.L., Appelo, C., 1999. User's Guide to PHREEQC (Version 2): A Computer Program for Speciation, Batch-reaction, One-dimensional Transport, and Inverse Geochemical Calculations. U.S. Geological Survey : Earth Science Information Center.

Pina, C.M., 2015. Reaction pathways toward the formation of dolomite. Am. Mineral. 100, 1017–1018. http://dx.doi.org/10.2138/am-2015-5269.

Plummer, L.N., Busenberg, E., 1982. The solubilities of calcite, aragonite and vaterite in CO_2-H_2O solutions between 0 °C and 90 °C, and evaluation of the aqueous model for the system $CaCO_3$-CO_2-H_2O. Geochim. Cosmochim. Acta 46, 1011–1040. http://dx.doi.org/10.1016/0016-7037(82)90056-4.

Purgstaller, B., Konrad, F., Dietzel, M., Immenhauser, A., Mavromatis, V., 2017. Control of Mg^{2+}/Ca^{2+} activity ratio on the formation of crystalline carbonate minerals via an amorphous precursor. Cryst. Growth Des. 17, 1069–1078. http://dx.doi.org/10.1021/acs.cgd.6b01416.

Reddy, M.M., Wang, K.K., 1980. Crystallization of calcium-carbonate in the presence of metal-ions: I. Inhibition by magnesium-ion at ph 8.8 and 25 °C. J. Cryst. Growth 50, 470–480. http://dx.doi.org/10.1016/0022-0248(80)90095-0.

Rinaldi-Montes, N., González-López, J., Fernández-González, A., Jiménez, A., Martínez-Blanco, D., Amghouz, Z., Gorria, P., Blanco, J.A., 2017. Lamellar Co_3O_4 nanoparticles recycled from synthetic cobalt carbonate: core/shell morphology and magnetic properties. Ceram. Int. 43, 10889–10894. http://dx.doi.org/10.1016/j.ceramint.2017.05.125.

Rodriguez-Blanco, J.D., Shaw, S., Bots, P., Roncal-Herrero, T., Benning, L.G., 2014. The role of Mg in the crystallization of monohydrocalcite. Geochim. Cosmochim. Acta 127, 204–220. http://dx.doi.org/10.1016/j.gca.2013.11.034.

Rodriguez-Navarro, C., Cara, A.B., Elert, K., Putnis, C.V., Ruiz-Agudo, E., 2016. Direct nanoscale imaging reveals the growth of calcite crystals via amorphous nanoparticles. Cryst. Growth Des. 16 (4), 1850–1860. http://dx.doi.org/10.1021/acs.cgd.5b01180.

Rodriguez-Navarro, C., Kudlacz, K., Cizer, O., Ruiz-Agudo, E., 2015. Formation of amorphous calcium carbonate and its transformation into mesostructured calcite. CrystEngComm 17, 58–72. http://dx.doi.org/10.1039/c4ce01562b.

Sánchez-Pastor, N., Gigler, A.M., Cruz, J.A., Park, S.H., Jordan, G., Fernández-Díaz, L., 2011. Growth of calcium carbonate in the presence of Cr(VI). Cryst. Growth Des. 11, 3081–3089.

Taylor, G.F., 1975. Occurrence of monohydrocalcite in 2 small lakes in southeast of South-Australia. Am. Mineral. 60, 690–697.

Wada, N., Yamashita, K., Umegaki, T., 1995. Effects of divalent cations upon nucleation, growth and transformation of calcium carbonate polymorphs under conditions of double diffusion. J. Cryst. Growth 148, 297–304.

Zhang, Z., Xie, Y., Xu, X., Pan, H., Tang, R., 2012. Transformation of amorphous calcium carbonate into aragonite. J. Cryst. Growth 343, 62–67. http://dx.doi.org/10.1016/j.jcrysgro.2012.01.025.